

Site percolation thresholds and universal formulas for the Archimedean lattices

Paul N. Suding and Robert M. Ziff†

Department of Chemical Engineering, University of Michigan, Ann Arbor, MI 48109-2136

(June 12, 2018)

Abstract

The site percolation thresholds p_c are determined to high precision for eight Archimedean (uniform) lattices, by the hull-walk gradient-percolation simulation technique, with the results $p_c = 0.697\,043$, honeycomb or (6^3) , $0.807\,904$ $(3, 12^2)$, $0.747\,806$ $(4, 6, 12)$, $0.729\,724$ $(4, 8^2)$, $0.579\,498$ $(3^4, 6)$, $0.621\,819$ $(3, 4, 6, 4)$, $0.550\,213$ $(3^3, 4^2)$, and $0.550\,806$ $(3^2, 4, 3, 4)$, and errors of about $\pm 2 \times 10^{-6}$. (The remaining Archimedean lattices are the square (4^4) , triangular (3^6) and Kagomé $(3, 6, 3, 6)$, for which p_c is already known exactly or to a high degree of accuracy.) The numerical result for the $(3, 12^2)$ lattice is consistent with the exact value $[1 - 2 \sin(\pi/18)]^{1/2}$, which we also derive. The values of p_c for all Archimedean lattices are found to be linearly related to the density of sites within an error of about 1%, which is more accurate than correlations based solely upon the coordination number. Comparison with nonuniform lattices is also made.

PACS numbers(s): 64.60Ak, 05.70.Jk

Typeset using REVTeX

I. INTRODUCTION

The Archimedean (Arch) tilings were first elucidated and published by Kepler (a translation of which can be found in [1]). These lattices received their name from references in Kepler's paper to Archimedes' descriptions of regular solid polyhedra, which are related to these 2d lattices. The significance of the Arch tilings or lattices, which are shown in Fig. 1, is that they are the complete set of lattices having infinite tessellation in which all vertices are equivalent. (They are also called "uniform" lattices.) This property has made them useful in the study of mathematics [2], crystallization [3,4], statistical mechanics [5], as well as percolation [6]. The familiar square, triangular, honeycomb and Kagomé lattices are all Arch.

The primary goal of this study was to determine precise values of the site percolation threshold p_c for all Arch lattices for which accurate values were not previously known. A few years ago, d'Iribarne, et al. determined p_c for all but one of the Arch lattices (which they call "mosaics") to about three significant figures [6], using a method based upon the analysis of the minimum spanning tree of clusters [7]. More recently van der Marck (vdM) [8,9] determined the thresholds for three of these lattices to nearly four figures. Furthermore, the threshold for the honeycomb lattice, a common one for percolation studies, was previously known only to about four figures [9,12,13]. Here, we extend the precision of these thresholds to six significant figures. We did not consider the square, triangular, and Kagomé lattices, as $p_c(\text{site})$ is either known exactly (triangular and Kagomé [14]), or has already been measured to a high degree of precision (square [15]) for these cases.

The second goal of this study was to explore the dependence of p_c upon lattice characteristics and determine to what extent a universal formula can be found for 2d site percolation. Recently there has been renewed interest in this question with the extensive work of Galam and Mauger (GM) [16–20] and vdM [8,9,22–24]. The Arch lattices provide an excellent resource for studying this question because they possess a range of coordination numbers from 3 to 6 and a variety of other lattice characteristics.

A. Nomenclature

Unfortunately, neither Kepler nor Archimedes (nor anyone else to our knowledge) assigned common names to all the Arch lattices. However, Grünbaum and Shephard [25] have introduced a general notation, which we use here, to categorize such lattices in terms of the set of polygons which surround each vertex, $(n_1^{a_1}, n_2^{a_2}, \dots)$. Going clockwise around a vertex, the numbers n_i denote the number of sides of each polygon, and the superscript a_i refers to the number of these polygons adjacent to each other. For example, the triangular lattice has six triangles around a given point, and is designated (3^6) . The labels for all the Arch lattices are shown in Fig. 1. Note that the $(3, 12^2)$ lattice has been called the “3-12” lattice in the literature, and in places the $(4, 8^2)$ has been given the name of “bathroom tile” lattice.

For convenience in our work we did assign nicknames to the lattices, which are listed in Table I. The $(4, 6, 12)$ is called the “cross” lattice because of the cross in Fig. 3; the $(4, 8^2)$ lattice is named after our local shopping mall, Briarwood, which (like many such malls) has tiles of this shape on its floor; $(3^3, 4^2)$ is called the “direct” lattice because of its directed structure, etc. The origins of the rest of the names are, we hope, somewhat more obvious.

II. METHOD

A. Hull Gradient Walk

To find p_c we employ the hull-gradient method [26], which we previously used to determine p_c for site percolation on the square lattice [27] and for bond percolation on the Kagomé lattice [28], both to more than six significant digits of precision.

In gradient percolation [29,30], a linear gradient of occupied sites is applied in the vertical direction of the lattice. As the height increases, the concentration of occupied sites also increases. This gradient forms two “land masses” within the lattice: a continuous region of occupied sites located at the top of the lattice and a continuous region of vacant sites

located at the bottom (Fig. 2). The boundary between these two regions forms a path whose average height provides an estimate for p_c .

To make this method efficient for finding p_c , we employ a hull-generating walk [31,32] which simultaneously generates and identifies the interfacial boundary. The status (whether occupied or vacant) of a site encountered by the walk is determined by generating a random number and comparing that number with the occupation probability for that height. If the walk does not arrive at a given site, the status of that site will not be determined, and no random number will be generated for it, contributing to the efficiency. In fact, we believe that the hull-gradient method is the most efficient way to determine p_c for 2d lattices. It is also quite simple to program, as it involves no lists or cluster labelling algorithms.

For each gradient $|\nabla p|$, an estimate of p_c may also be obtained by taking the ratio of occupied to total (occupied plus vacant perimeter) sites belonging to the hull [30]. As the size of the system is increased or the gradient is decreased, $p_c(|\nabla p|)$ approaches p_c linearly in $|\nabla p|$. Thus a simple extrapolation of the data for finite gradients gives the infinite-system value. In practice, we considered gradients sufficiently small (typically of the order of $10^{-4} \Delta p/\text{lattice spacing}$) that the extrapolation from the final point to zero gradient was of the order of the error bars of that last point. Additional details of the method are given in [26,28].

B. Computer Techniques

In the simulation, the status of all points visited by the walk must be stored in computer memory. To accomplish this efficiently, all of the Arch lattices were transformed to align on rectilinear grids, as shown in Fig. 3. Note that the gradient was not applied directly to these squared-off forms, as some lattices had to be distorted in the vertical direction to get them in this form. Instead, all numerical calculations were performed so that the height of the point in the original, undistorted, lattice was used to find $p(z)$. Previously we showed, for bond percolation on the Kagomé lattice, that assigning $p(z)$ this way yields the best linear

scaling of p_c vs. gradient [28]. For two lattices, we considered two possible orientations of the lattice and found similar results, as discussed in Appendix A.

The lattices were initialized by filling the top half of the first column with occupied sites and the lower half with vacant sites, which prevents the walk from closing on itself at the start of the algorithm (Fig. 2). Periodic boundary conditions were applied in the horizontal direction, and each new column to the right was cleared as it was visited. This allowed the simulation to run indefinitely and have essentially no boundary effects from the horizontal ends of the system. The maximum distance the walk traveled horizontally from the front was tracked to detect if wraparound errors occurred; if they did, the system size and/or gradient was adjusted accordingly, and the run was restarted with the expanded system.

Random numbers were generated using the shift-register sequence generator R7(9689) [33,34] defined by:

$$x_n = x_{n-471} \wedge x_{n-1586} \wedge x_{n-6988} \wedge x_{n-9689} , \quad (1)$$

where \wedge is the bitwise exclusive-or operation. This ‘four tap’ generator is equivalent to decimating by 7 (taking every seventh term) of the sequence generated by the two-tap rule R(9689) ($x_n = x_{n-471} \wedge x_{n-9689}$) given by Zierler [35], where the decimation has the effect of greatly reducing the three- and four-point correlations of the two-tap generator [33]. Our previous work has shown that this generator does not appear to introduce errors in simulations of this kind [26,28].

III. RESULTS AND DISCUSSION

A. Percolation thresholds

For each lattice, p_c was plotted as a function of the gradient. Fig. 4 shows a representative plot for the $(3, 12^2)$ lattice. In all cases, a linear relationship was observed between the magnitude of the gradient and the estimate $p_c(|\nabla p|)$, as found previously for the square [30] and Kagomé lattices [28]. The value at the intercept of the y -axis represents p_c for an

infinite lattice (zero gradient), and these values are reported in Table I. Also shown in Table I is the quantity of random numbers generated for each simulation, which is identical to the total number of occupied and vacant sites belonging to the hull, because one random number is generated for each new site visited. These simulations consumed several months of computer time on Sun and HP workstations.

For all our values, the error (which is purely statistical in origin) is of order 10^{-6} . Our results are consistent with d'Iribarne et al.'s three-digit values, if we assume an error of ± 0.003 in their data. Our result $0.697043(2)$ for the honeycomb lattice is consistent with the previous values $0.6973(8)$ of Vicsek and Kertész [12], $0.6962(6)$ of Djordjevic et al. [13], and $0.6971(2)$ of vdM [9]. Likewise, our results agree with the determinations $0.5504(2)$ for $(3^3, 4^2)$ and $0.7298(1)$ for $(4, 8^2)$ made recently by vdM [8,10].

In another recent work, Pr ea [36] has calculated the distance sequences c_n , defined as the number of sites n steps (chemical distance) from the origin, for the Arch lattices. Pr ea found a monotonic relation between $p_c(\text{site})$ and $c \equiv \lim_{n \rightarrow \infty} \inf(c_n/n)$, although three different lattices with different p_c — the square, Kagom e, and $(3, 4, 6, 4)$ — share the same value $c = 4$. This apparent monotonic behavior led Pr ea to conjecture that p_c for the $(3^4, 6)$ lattice (the one Arch lattice not studied previously) is within in interval $(0.55, 0.6)$. Our result $0.579498(2)$ confirms this conjecture.

B. Exact percolation threshold for the $(3, 12^2)$ lattice

The threshold for the $(3, 12^2)$ can be derived exactly. The proof is based upon the similarity of structure between this lattice and the Kagom e lattice. In Fig. 5, the $(3, 12^2)$ lattice is shown with the triangle bonds in bold and the bonds between the triangles as dashed lines. If the dashed lines are reduced in length, the $(3, 12^2)$ lattice transforms into the Kagom e lattice. Similarly, the sites on both ends of the dashed line in the $(3, 12^2)$ (marked by the large circle in the figure), taken together, are equivalent to a single point on the Kagom e lattice.

Let both lattices be at the percolation threshold and p be the probability that a given site on the $(3, 12^2)$ lattice is occupied. Then, p^2 is the probability that both sites at the ends of the dashed bonds are occupied, and the bond will permit flow. The dashed bond is equivalent to a single point on the Kagomé. At the percolation threshold, the probability that a site is occupied on the Kagomé lattice is $1 - 2 \sin(\pi/18)$. Therefore, for the $(3, 12^2)$ lattice,

$$p_c = [1 - 2 \sin(\pi/18)]^{1/2} = 0.807\,900\,764\dots \quad (2)$$

Our numerical estimate 0.807904 is consistent with this result within the error bars $\pm 0.000\,003$. This agreement provides a further validation of both our algorithm and error analysis.

C. Galam and Mauger's universal formula for p_c

Early in the work of percolation, thresholds were related with coordination number q using relatively simple formulas. More recently, GM [20,19] have attempted to refine this by introducing different classes of lattices, characterized by the constants p_0 , a and b in their formula

$$p_c = p_0[(d-1)(q-1)]^{-a} d^b, \quad (3)$$

where d is the dimensionality. By defining two different classes, each with distinct sets of constants p_0 and a for site and bond percolation (with $b = a$ for bond and $b = 0$ for site percolation), GM were able to obtain a fairly good fit of p_c for a number of lattices of various dimensionality, with a fifth set of constants p_0 and a required for systems of very high dimensionality. Their class 1 contains all 2d lattices except the Kagomé, while class 2 comprises all higher-dimensional systems plus the 2d Kagomé.

Subsequently, vdM [8,22] considered a number of additional lattices and argued that a formula of this type, depending only upon d and q , cannot be very accurate because of the

existence of different lattices with differing p_c but identical d and q . GM [19] responded that their formula is applicable only for “isotropic” lattices in which each site has the identical q . (In this present paper, we describe these lattices as “uniform,” by which we mean that each vertex is identical in terms of its surrounding polygons, allowing for rotations and reflections.) For other lattices, GM reformulated (3) by reinterpreting q to be an effective coordination number q_{eff} (not necessarily the average value \bar{q}). Because q_{eff} cannot be found independently, this reinterpretation has the effect of turning their formula into a correlation between site and bond thresholds for a given lattice rather than a more general correlation for p_c , which is developed further in [21] and discussed in [9,11]. However, because we do not consider thresholds for bond percolation here, we do not address this aspect of GM’s work in this paper.

In Fig. 6 we plot our results using the same axes as GM [20], $\ln(1/p_c)$ vs. $\ln(q-1)$. We also exhibit GM’s two fitting formulas for site percolation, which are straight lines on this plot. Clearly, many of the Arch lattices do not fall near either of these two lines. Evidently, GM’s approach (3) cannot accommodate these additional uniform lattices, unless one introduces still more lattice classes, which is counter to the concept of universality.

D. A new fitting formula for p_c

For the Arch lattices, one can observe the trend that p_c increases with increasing “openness” of the lattices. To characterize the latter, we introduce the quantity ρ equal to the density or number of lattice sites per unit area, assuming that all bond lengths are unity. Its inverse, the area per site, can be determined by drawing lines which bisect the centers of each polygon surrounding a given site, as in a dual-lattice construction, and summing the enclosed area. The tiles defined by these bisector lines clearly fill the entire lattice. The total area per site is simply 1/3 the area of each triangle, 1/4 the area of each square, etc., surrounding that site. For Arch lattices with uniform bond lengths, all polygons are regular. The area of $1/n$ -th of a regular n -gon, with unit edge length, is given by

$$A_n = \frac{1}{4} \cot \frac{\pi}{n} , \quad (4)$$

with some numerical values given in Table II. For a lattice characterized by vertices $(n_1^{a_1}, n_2^{a_2}, \dots)$, we then have

$$\rho = \left[\sum_i a_i A_{n_i} \right]^{-1} = 4 \left[\sum_i a_i \cot \frac{\pi}{n_i} \right]^{-1} . \quad (5)$$

The resulting values of ρ for the Arch lattices are listed in Table III. In Fig. 7 we show a plot of p_c vs. ρ , and indeed one can see that the correlation between p_c and ρ is good. Furthermore, that correlation can be well represented by a simple linear function. A least-squares fit yields

$$p_c = 1.0405 - 0.4573\rho . \quad (6)$$

The errors involved in using this formula are listed in the column Δ in Table III, and are generally within about 0.01, in contrast to errors up to 0.05 if GM's correlations were used (taking the best class in each case). In Fig. 8 we plot the errors from using these different fitting formulas for the various lattices, clearly showing how GM's formulas are each accurate for certain lattices only, while (6) works fairly well for all of the lattices. The rms errors from using (6) for the 11 Arch lattices equals 0.0075.

It turns out that our fit (5-6) is related to a correlation for p_c given by Scher and Zallen nearly three decades ago [39]. These authors introduced a ‘‘filling factor’’ f defined as the fraction of space occupied by disks of radius 1/2 placed at each lattice site, and found for four lattices in 2d,

$$fp_c \approx \text{const.} = 0.44 \pm 0.02 . \quad (7)$$

Now, f is simply $\pi\rho/4$, so that their correlation also relates to the density of sites. However, while their hyperbolic relation (7) provided a good fit to lattices they considered (to the accuracy available at that time), it does not capture the behavior for the other lattices, especially those of low ρ , as shown in Fig. 7, where (7) is also plotted.

Fairly recently, d'Iribarne et al. [6] considered a correlation for p_c of the Arch lattices that is also closely related to ρ or f . They compared p_c to a variable m which represents the average edge length of a minimally spanning tree on a complete lattice, normalized by the area. Because on the complete graph there is one edge per site, m is identical to $\rho^{1/2}$. Their plot of p_c vs. m correlates the data to a single curve just as our Fig. 7 does, however, in terms of m the behavior is quite curved, which d'Iribarne et al. fit to the quadratic

$$p_c = 0.685 + 0.799m - 0.899m^2 . \quad (8)$$

In fact, this fit reduces the rms error of our results over the 11 lattices to 0.0057. (Note, only a slight improvement is obtained by adjusting these coefficients for our new values of p_c .) However, the expense of this improvement is an extra parameter in (8) over (6). Indeed, one can also extend (6) to a quadratic in ρ , with the result

$$p_c = 0.9472 - 0.2181\rho - 0.1439\rho^2 , \quad (9)$$

which gives a comparable rms error over the 11 lattices, 0.0054, but again at the expense of a more complicated formula than (6).

Along these lines, it is interesting to note that an excellent fit can be achieved using results from only the three lattices where p_c is known exactly (which happen to span the whole range of p_c values). That fit,

$$p_c = 0.9466 - 0.1972\rho - 0.1642\rho^2 , \quad (10)$$

yields an rms error over the 11 Arch lattices of 0.0062, only slightly worse than (8) or (9). This fitting formula depends upon no adjustable parameters nor any Monte-Carlo-measured values.

E. Extension to non-uniform lattices

We have found that (5-6) may also be applied to non-uniform lattices, if in calculating ρ by (5), a_n is interpreted as the *average* number of polygons of type n over all vertices. For

the non-uniform lattices (also referred to as anisotropic [20]), many of the polygons are not regular, and it is not always possible to make all bonds of the same length, which were the two assumptions in deriving (5). Thus, we now consider (5) to represent a topological or graphical weight rather than an actual geometric property of the lattices.

We looked at seven non-uniform lattices considered by vdM [8,9] and/or GM [20] and whose values of p_c are known (we did not determine any of these p_c 's here): the bowtie, bowtie dual, pentagonal, $(4, 8^2)$ -matching, dice, Penrose, and Penrose dual lattices. The first five of these lattices are shown in Fig. 9, while the quasicrystalline Penrose and Penrose dual are shown for example in [38] and [20]. The form of the Penrose lattice used here is the rhomb or P3 form [25].

For the dice lattice, $\frac{1}{3}$ of the vertices are (4^6) while $\frac{2}{3}$ of them are (4^3) , so on the average the vertices are (4^4) . Likewise for the $(4, 8^2)$ -matching, we have $\frac{1}{3}(3^2, 8^2) + \frac{2}{3}(3^2, 4, 8) = (3^2, 4^{2/3}, 8^{4/3})$, for the bowtie $\frac{1}{2}(3^4, 4^2) + \frac{1}{2}(3^2, 4^2) = (3^3, 4^2)$, for the bowtie dual $\frac{1}{3}(4^2, 6^2) + \frac{2}{3}(4, 6^2) = (4^{4/3}, 6^2)$, and for the pentagonal $\frac{1}{3}(5^4) + \frac{2}{3}(5^3) = (5^{10/3})$. For the Penrose lattice, the average vertices are simply (4^4) , while for the Penrose dual lattice the average vertices are [40] $(3^{a_3}, 4^{a_4}, 5^{a_5}, 6^{a_6}, 7^{a_7})$ with $a_3 = 3(x^2 + x^4) = 3(3 - 4x) = 1.583592135$, $a_4 = 4x^5 = 4(5x - 3) = 0.360679775$, $a_5 = 5(x^3 + x^6) = 5(4 - 6x) = 1.458980338$, $a_6 = 6x^7 = 6(13x - 8) = 0.206651122$, and $a_7 = 7x^6 = 7(5 - 8x) = 0.39009663$, where $x = (\sqrt{5} - 1)/2$ is the inverse of the golden ratio. Note that in general a_n satisfy $\sum_n (1 - 1/n)a_n = 1$ and $\sum_n a_n = \bar{q}$, where \bar{q} is the average coordination number.

These average vertex numbers are listed in Table IV, along with p_c values, ρ values, p_c^{est} and error Δ from using (5-6). Interestingly, the Δ for all 7 of these lattices are generally smaller than those for the Arch lattices — with an rms value of 0.0046 vs. 0.0075. (Note that some of these Δ 's are however close to the precision of the value of p_c .) Surprisingly, even the Penrose dual lattice, which incorporates polygons with from 3 to 7 sides and a very irregular structure, is also well modelled by this formula. Evidently, this approach, which is based upon ρ given by (5), appears to be quite robust.

One could conceivably use these additional data points from the non-uniform lattices to

refine the fit of the formulas for $p_c(\rho)$ in Section III D. However, the improvement turns out to be marginal, and considering the relatively low precision of the values of p_c for the non-uniform lattices, the justification for doing this is doubtful.

Note that if one retained the definition of ρ literally as the density of sites for these lattices, rather than using the definition above, then the fit of the non-uniform lattices with (6) would be very poor. An example is given by the dice lattice, which has a site density identical to that of the triangular lattice, $2\sqrt{3}/3 = 1.1547$. The p_c for this lattice, 0.5851 [8], is substantially above the value for the triangular, $1/2$, and the data point for this case would fall well above the line in Fig. 7.

It is also interesting to note that we have now considered three different lattices with the same average vertex environment of three triangles and two squares: the two Arch lattices $(3^3, 4^2)$ and $(3^2, 4, 3, 4)$, and the non-uniform bowtie lattice, which have p_c 's of 0.550 806, 0.550 213, and 0.5475(8) respectively. The closeness of these values supports the idea that p_c is determined principally by the local nature of the lattice as characterized by the vertex numbers. For the two Arch lattices, the p_c 's are nearly identical, and close to the prediction by (6) of 0.5503. The bowtie lattice, which has the same vertex numbers as the others on the average only, has a value of p_c that is slightly lower, by about 0.003.

The inadequacy of using q alone to estimate p_c is also apparent, as the $(3^4, 6)$ lattices has the same $q = 5$ as these three above, but a p_c that is substantially higher, 0.579 498. The results for the non-uniform lattices are also included in Fig. 6, using \bar{q} for q .

A similar situation occurs for the square ($p_c = 0.592 746$), dice ($p_c = 0.5848$), and Penrose ($p_c = 0.5837$) lattices, whose (average) vertices are (4^4) in all cases. Again, the non-uniform lattices have a slightly lower p_c than the uniform one with the same vertices, with the “most” non-uniform one (the Penrose) having the lowest p_c . And again, other lattices with $q = 4$ but different average vertex numbers (there are four of them here) all have much different (and higher) p_c 's.

van der Marck has pointed out [23,10] that adding an extra site at the center of any triangle on a 2d lattice does not change the value of p_c (site). If these extra sites are

included in the calculation of ρ , then ρ would change and the predictions of 6 would be poor. Therefore, in applying these formulas, one must disregard these superfluous sites. However, there are undoubtedly other classes of lattices where 5-6 will not work well — and will not be so easily fixed.

F. Further variations on the fitting formula

Although a precise universal formula for p_c based upon the vertex numbers alone is impossible, it is interesting to explore variations to (5-6) to see what improvements can be made. According to (5), the variable ρ^{-1} is an average over the nearest neighbors polygons weighted by A_n . To see how close this weighting compares to an optimal one, we carried out a regression analysis, allowing all A_n as well as the linear fit of $p_c(\rho)$ to vary, and minimizing the error from the linear fit using data from all 18 lattices given above, both Arch and non-uniform. This procedure yielded the A'_n given in Table II and the fit

$$p_c = 1.1383 - 0.5503\rho', \quad (11)$$

where $\rho' = \sum a_n A'_n$. Note that we kept $A'_4 = 0.25$, as one weight can be fixed arbitrarily.

The errors using this fit are generally lower than those that result from (6); in fact the rms error over all 18 lattices decreases substantially from 0.0065 when (6) is used to 0.0028 when (11) is used. However, this formula is clearly less predictive than eq. (6), which had no adjustable parameters in the definition of ρ .

The A'_n listed in Table II fall close to, but in a somewhat narrower range than, the A_n . (Note A'_7 is somewhat out of line with the rest, being bigger than A_7 , but was derived from only one lattice, the Penrose dual.) These results suggest that there might be a topological weighting rule that is better than the effective area per site, (5). However, we do not know what that weighting rule may be.

To test if a non-linear relation between p_c and ρ' may be better, we carried out the same regression analysis as above, but allowed for a quadratic $p_c(\rho)$. Interestingly, the A'_n came out nearly the same, and the behavior of $p_c(\rho)$ was very nearly linear.

Using d'Iribarne et al.'s form (8), with $m = \sqrt{p'}$ as the variable and assuming a quadratic relation between p_c and m , we found optimal weights A'_n now much closer to the A_n . These various and partly contradictory results suggest that, while some improvements can be made, our original assumptions — that A_n is the actual polygon area, and that $p_c(\rho)$ is linear — are not unreasonable.

Of course, there are deeper assumptions to this whole approach — that ρ^{-1} is a linear function of the a_n , and that p_c is a simple linear or quadratic function of ρ — which we have not explored. And ultimately, to get a more precise formula for p_c , one must also take into account the actual arrangement of the polygons around each vertex, not just the number of each type of polygon. Clearly, further work can be done in understanding the relation of p_c to lattice type.

G. Conclusions

We have determined the $p_c(\text{site})$ for the honeycomb and seven less-common Arch lattices to nearly six significant figures, about 100 to 1000 times more precise than previously known — except for the $(3^4, 6)$ lattice, whose p_c was never determined previously. The value for the latter lattice is within the conjectured bounds of Pr ea [36]. We find a fairly good linear correlation between p_c and ρ (and related to the correlations of Scher and Zallen [39] and of d'Iribarne et al. [6]), although its accuracy is far below what can be found in simulation. This correlation can be extended to non-uniform lattices, and can be improved somewhat if the weightings A_n are adjusted to the A'_n . The correlation with ρ is substantially more accurate than correlations based primarily upon coordination number, such as those of GM [16–18].

All our results here are restricted to 2d and to site percolation. It would be interesting to see if these ideas on relating p_c to the local graphical environment can be extended to bond percolation and to higher dimensionality. It would also be interesting to see how well GM's ideas relating $p_c(\text{site})$ and $p_c(\text{bond})$ on the same lattices hold for the Arch lattices.

ACKNOWLEDGMENTS

The authors thank Steven van der Marck for comments and for providing unpublished improved p_c values for some non-uniform lattices. This material is based upon work supported by the US National Science Foundation under Grant No. DMR-9520700, and by the Shell Oil Company Foundation.

APPENDIX A: IMPORTANCE OF GRADIENT ORIENTATION

In order to verify that the direction that the gradient is applied on a lattice has no effect on p_c , we calculated p_c for both the honeycomb and $(3^3, 4^2)$ lattices after they had been rotated 90 degrees. Fig. 10 shows the original orientation of the simulation and the orientation after the lattice has been rotated 90 degrees. The p_c for the honeycomb lattice was measured as $0.697\,043 \pm 0.000\,002$ and then $0.697\,046 \pm 0.000\,003$ after 90 degree rotation. Likewise, for the $(3^3, 4^2)$ lattice, p_c was measured as $0.550\,213 \pm 0.000\,002$ and then $0.550\,211 \pm 0.000\,002$ after 90 degree rotation. In both cases, the p_c values were identical within the error of the method, verifying that the orientation of the lattice has no effect on determining p_c in our method.

[†]Electronic mail: rziff@engin.umich.edu

REFERENCES

- [1] J. V. Field, *Vistas in Astronomy* **23**, 109 (1979); *Arch. Hist. Exact Sci.* **50**, 241 (1997).
- [2] L. Fejes Tóth, *Acta Mathematica* **11**, 363 (1960).
- [3] F. C. Frank and J. S. Kasper, *Acta Cryst.* **11**, 184 (1958); **12**, 483 (1959).
- [4] H. Takeda and J. D. H. Donnay, *Acta Cryst.* **19**, 474 (1965).
- [5] R. Shrock and S. H. Tsai, *Phys. Rev. E* **56**, 2733, 4111 (1997).
- [6] C. d'Iribarne, G. Rasigni and M. Rasigni, *Phys. Lett. A* **209**, 95 (1995).
- [7] C. Dussert, G. Rasigni and M. Rasigni, *Phys. Lett. A* **139**, 35 (1989).
- [8] S. C. van der Marck, *Phys. Rev. E* **55**, 1514 (1997); Erratum **56**, 3732 (1997).
- [9] S. C. van der Marck, *Int. J. Mod. Phys. C* **9**, 529 (1998).
- [10] S. C. van der Marck, Private communication.
- [11] F. Babalievski, preprint cond-mat/9711164.
- [12] T. Vicsek and J. Kertész, *Phys. Lett.* **81A**, 51 (1981).
- [13] Z. V. Djordjevic, H. E. Stanley and A. Margolina, *J. Phys. A: Math. Gen.* **15**, L405 (1982).
- [14] J. W. Essam and M. F. Sykes, *J. Math. Phys. (N. Y.)* **5**, 1117 (1964).
- [15] R. M. Ziff, *Phys. Rev. Lett.* **69**, 2670 (1992).
- [16] S. Galam and A. Mauger, *J. Appl. Phys.* **75**, 5526 (1994).
- [17] S. Galam and A. Mauger, *Physica A* **205**, 502 (1994).
- [18] S. Galam and A. Mauger, *Phys. Rev. E* **53**, 2177 (1996).
- [19] S. Galam and A. Mauger, *Phys. Rev. E* **55**, 1230 (1997).

- [20] S. Galam and A. Mauger, Phys. Rev. E **56**, 322 (1997).
- [21] S. Galam and A. Mauger, Eur. Phys. J. B **1**, 255 (1998).
- [22] S. C. van der Marck, Phys. Rev. E **55**, 1228 (1997).
- [23] S. C. van der Marck, Phys. Rev. E **55**, 6593 (1997).
- [24] S. C. van der Marck, J. Phys. A: Math. Gen. **31**, 3449 (1998).
- [25] B. Grünbaum and G. C. Shephard *Tilings and Patterns* (New York: Freeman and Co., 1987).
- [26] R. M. Ziff and B. Sapoval, J. Phys. A: Math Gen. **18**, L1169 (1986).
- [27] R. M. Ziff and G. Stell, Univ. Mich. report 11-88 (1988).
- [28] R. M. Ziff and P. N. Suding, J. Phys. A: Math. Gen. **30**, 5351 (1997).
- [29] B. Sapoval, M. Rosso and J. F. Gouyet, J. Physique Lett. (Paris) **46**, L149 (1985).
- [30] M. Rosso, J. F. Gouyet and B. Sapoval, Phys. Rev. B **32**, 6053 (1986).
- [31] R. M. Ziff, P. T. Cummings and G. Stell, J. Phys. A: Math. Gen. **17**, 3009 (1984).
- [32] A. Weinrib and S. Trugman, Phys. Rev. B **31**, 2993 (1985).
- [33] R. M. Ziff, Comp. Phys. **12**, 385 (1998).
- [34] S. W. Golomb, *Shift Register Sequences* (San Francisco: Holden-Day, 1967).
- [35] N. Zierler, Inform. Control **15**, 67 (1969).
- [36] P. Pr ea, Math. Comput. Modelling **26**, 317 (1997).
- [37] J. C. Wierman, J. Phys. A: Math. Gen. **17**, 1525 (1984); **21**, 1487 (1988).
- [38] F. Yonezawa, S. Sakamoto, and M. Hori, Phys. Rev. B **40**, 636 (1989).
- [39] H. Scher and R. Zallen, J. Chem. Phys. **53** 3759 (1970).

[40] J. P. Lu and J. L. Birman, *J. Statis. Phys.* **46** 1057 (1987).

FIGURES

FIG. 1. The 11 Archimedean (Arch) lattices, in which all vertices are equivalent. Lattices are designated using the notation of Grünbaum and Shephard [23] as explained in the text.

FIG. 2. The hull-generating walk along a percolation gradient for the honeycomb lattice. Filled circles denote occupied sites and heavy lines show the hull of the percolating region. The arrow points to the starting point of the walk.

FIG. 3. The Arch lattices transformed to a square array, for use in the computer simulation. Some lattices were distorted in the vertical direction, but in all cases the actual lattice height, rather than the height in the square array, was used to determine the site occupation probability.

FIG. 4. Percolation threshold vs. lattice gradient for the $(3, 12^2)$ lattice. As the gradient becomes smaller, the lattice approaches infinite size. The percolation threshold can be estimated from the y -intercept of a linear regression of results from finite lattices.

FIG. 5. Derivation of the exact percolation threshold for the $(3, 12^2)$ lattice. Replacing the dashed bonds with single points leads to the Kagomé lattice.

FIG. 6. Thresholds plotted as $\ln 1/p_c$ vs $\ln (q - 1)$. (\bullet) regular lattices (from left to right: honeycomb, square and triangular), (\square) Kagomé, (\triangle) less-common Archimedean lattices, (\times) non-uniform lattices. Dashed line: GM's class 1 formula; solid line, GM's class 2 formula. Evidently, many lattices do not conform to GM's classification scheme.

FIG. 7. Percolation thresholds as a function of ρ , with the same symbols as in Fig. 6. The linear fit is given in eq. (6). Also shown are is correlation of Scher and Zallen, eq. (7) (dashed line).

FIG. 8. Error from using GM's class 1 formula (\square), class 2 formula (\triangle), and our fit (5-6) (\bullet), for the 18 lattices, plotted sequentially in the order they are listed in Tables III and IV respectively. Formulas (8), (9) or (11) improves the fit of (5-6) even further.

FIG. 9. Five of the non-uniform lattices used to test the fitting formulas.

FIG. 10. Two orientations for the $(3^3, 4^2)$ and honeycomb lattices used to test the influence of lattice orientation in our method of determining p_c .

TABLES

TABLE I. Measured values of p_c for site percolation on the Archimedean lattices. Lattice nicknames in quotes are ours.

Lattice	Measured p_c	Total Random Numbers Generated
$(3, 12^2)$ “star”	0.807 904(3)	4.1×10^{11}
$(4, 6, 12)$ “cross”	0.747 806(3)	2.6×10^{11}
$(4, 8^2)$ “Briarwood”	0.729 724(2)	2.6×10^{11}
(6^3) honeycomb	0.697 043(2)	4.0×10^{11}
$(3, 4, 6, 4)$ “bounce”	0.621 819(2)	2.9×10^{11}
$(3^4, 6)$ “bridge”	0.579 498(2)	2.9×10^{11}
$(3^2, 4, 3, 4)$ “puzzle”	0.550 806(2)	2.8×10^{11}
$(3^3, 4^2)$ “direct”	0.550 213(2)	2.9×10^{11}

TABLE II. Weights A_n (4), and optimized weights A'_n which yield the best linear fit of $p_c(\rho')$ over all 18 lattices.

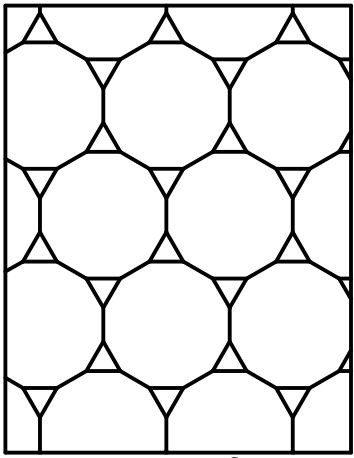
n	A_n	A'_n
3	0.144338	0.14400
4	0.25	0.25
5	0.344095	0.33640
6	0.433013	0.41653
7	0.519130	0.52539
8	0.603553	0.55041
12	0.933013	0.75490

TABLE III. Values of p_c and lattice characteristics for all 11 Arch lattices. Δ is the error when (6) is used to fit the data.

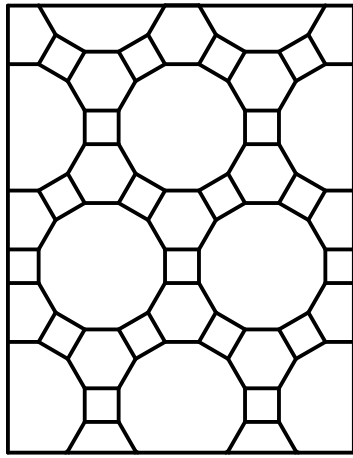
Lattice	p_c	Ref.	q	ρ by (5)	$p_c^{\text{est.}}$ by (6)	Δ
$(3, 12^2)$	0.807 904		3	0.4974	0.8130	-0.005
$(4, 6, 12)$	0.747 806		3	0.6188	0.7575	-0.010
$(4, 8^2)$	0.729 724		3	0.6863	0.7266	0.003
(6^3) honeycomb	0.697 043		3	0.7698	0.6885	0.009
$(3, 6, 3, 6)$ Kagomé	0.652 703 6	[14]	4	0.8660	0.6444	0.008
$(3, 4, 6, 4)$	0.621 819		4	0.9282	0.6160	0.006
(4^4) square	0.592 746 0	[15]	4	1	0.5832	0.010
$(3^4, 6)$	0.579 498		5	0.9897	0.5879	-0.008
$(3^2, 4, 3, 4)$	0.550 806		5	1.0718	0.5503	0.0005
$(3^3, 4^2)$	0.550 213		5	1.0718	0.5503	-0.0001
(3^6) triangular	0.5	[14]	6	1.1546	0.5124	-0.012

TABLE IV. Data for non-uniform lattices. Here vertex numbers represent averages.

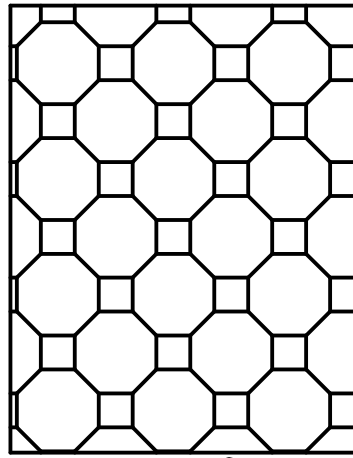
Lattice	p_c	Ref.	\bar{q}	ρ by (5)	$p_c^{\text{est.}}$ by (6)	Δ
$(4, 8^2)$ -matching $(3^2, 4^{\frac{2}{3}}, 8^{\frac{4}{3}})$	0.6768(2)	[8,10]	4	0.7936	0.6776	-0.0008
bowtie dual $(4^{\frac{4}{3}}, 6^2)$	0.6649(2)	[8,10]	$3\frac{1}{3}$	0.8338	0.6592	0.006
pentagonal $(5^{\frac{10}{3}})$	0.6476(2)	[9,10]	$3\frac{1}{3}$	0.8719	0.6418	0.006
Penrose dual (see text)	0.6381(3)	[38]	4	0.8987	0.6295	0.009
dice (4^4)	0.5848(2)	[8]	4	1	0.5832	0.002
Penrose (4^4)	0.5837(3)	[38]	4	1	0.5832	0.0005
bowtie $\bowtie (3^3, 4^2)$	0.5474(2)	[8,10]	5	1.0718	0.5503	-0.003



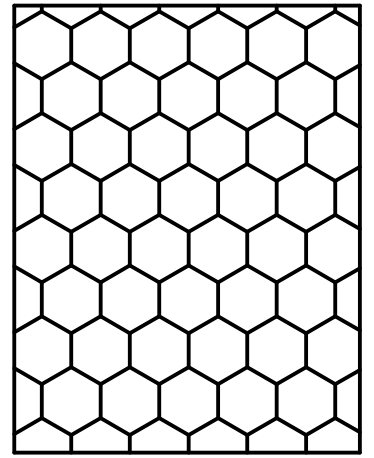
3.12^2



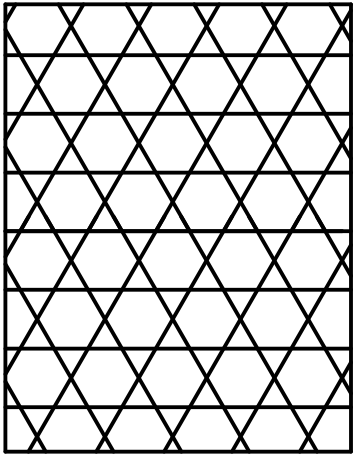
4.6.12



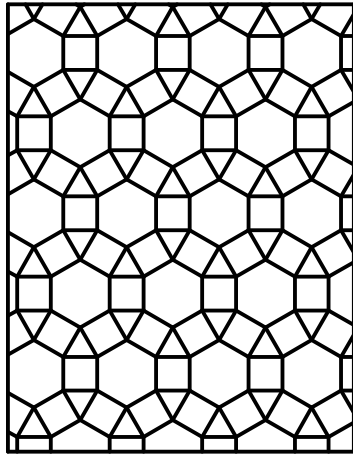
4.8^2



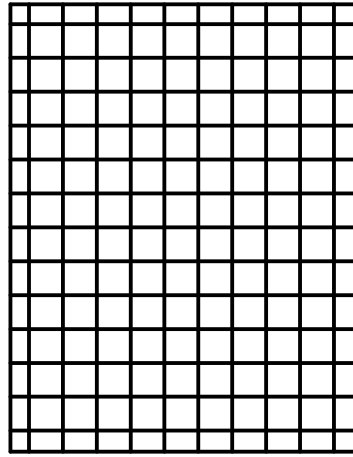
Honeycomb



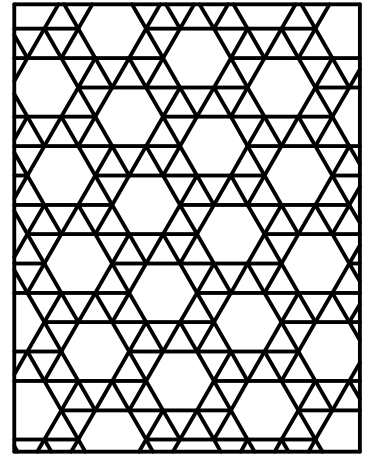
Kagome



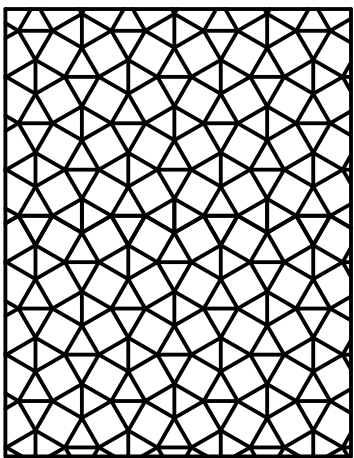
3.4.6.4



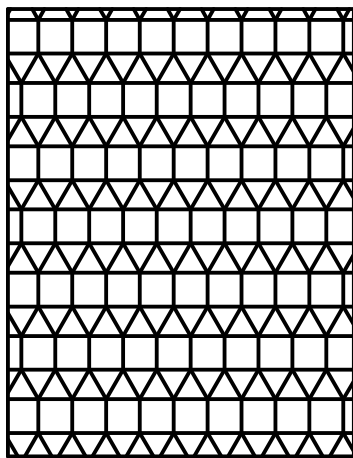
Square



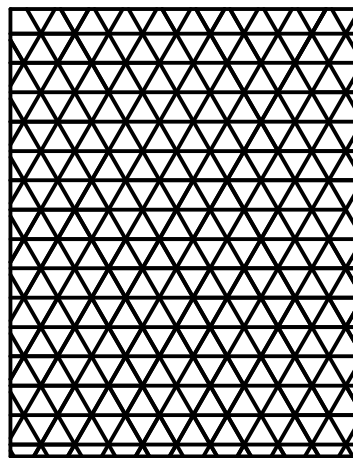
$3^4.6$



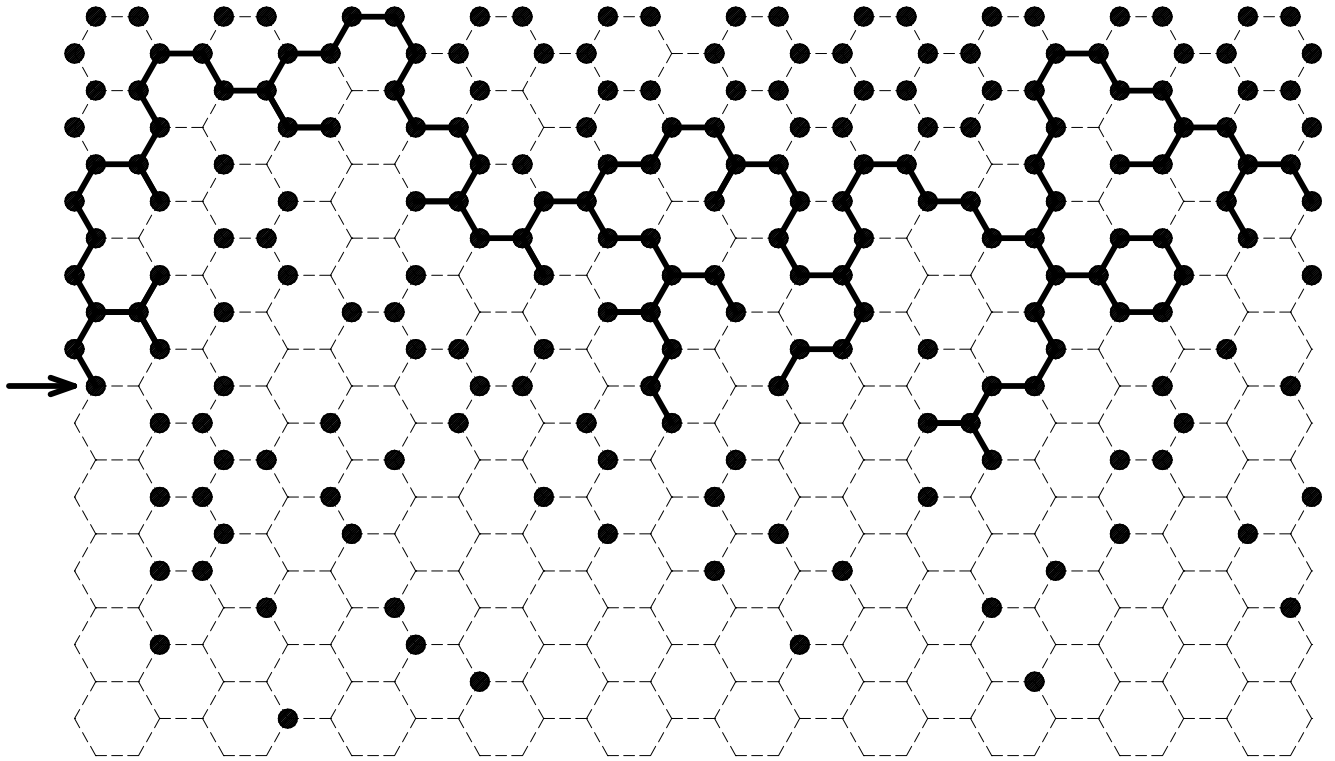
$3^2.4.3.4$

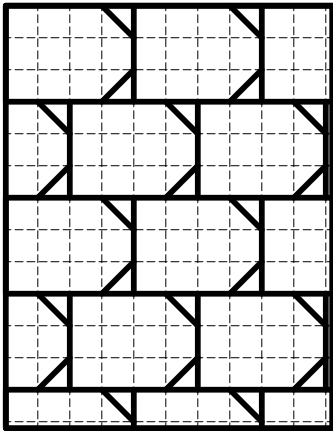


$3^3.4^2$

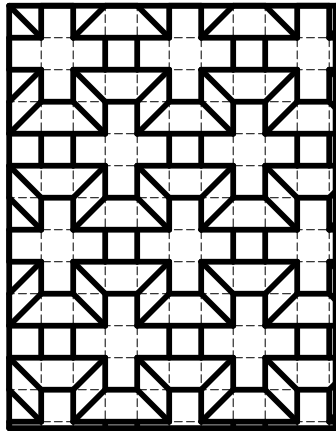


Triangular

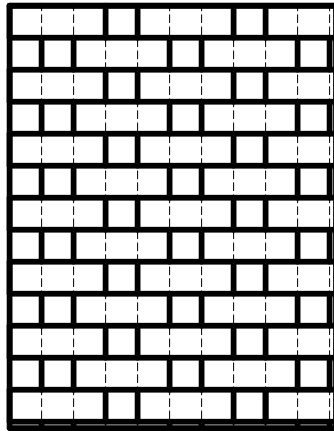




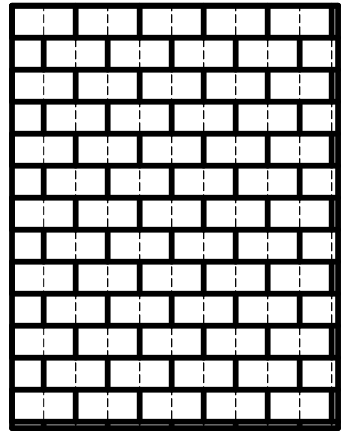
3.12^2



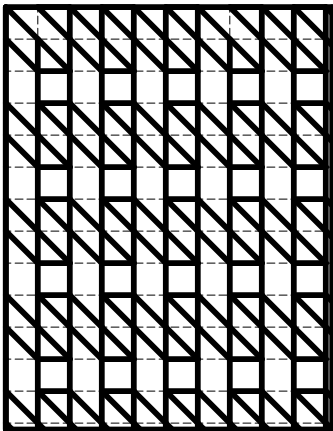
4.6.12



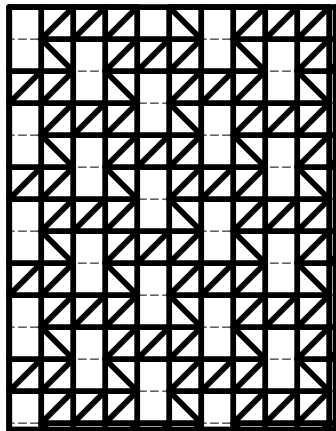
4.8^2



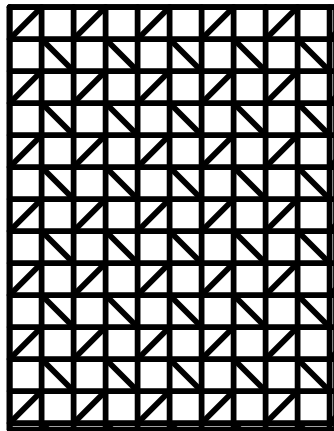
Honeycomb



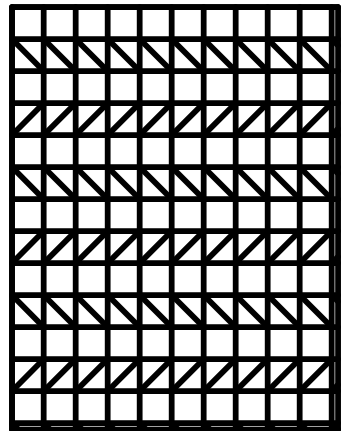
3.4.6.4



3^4

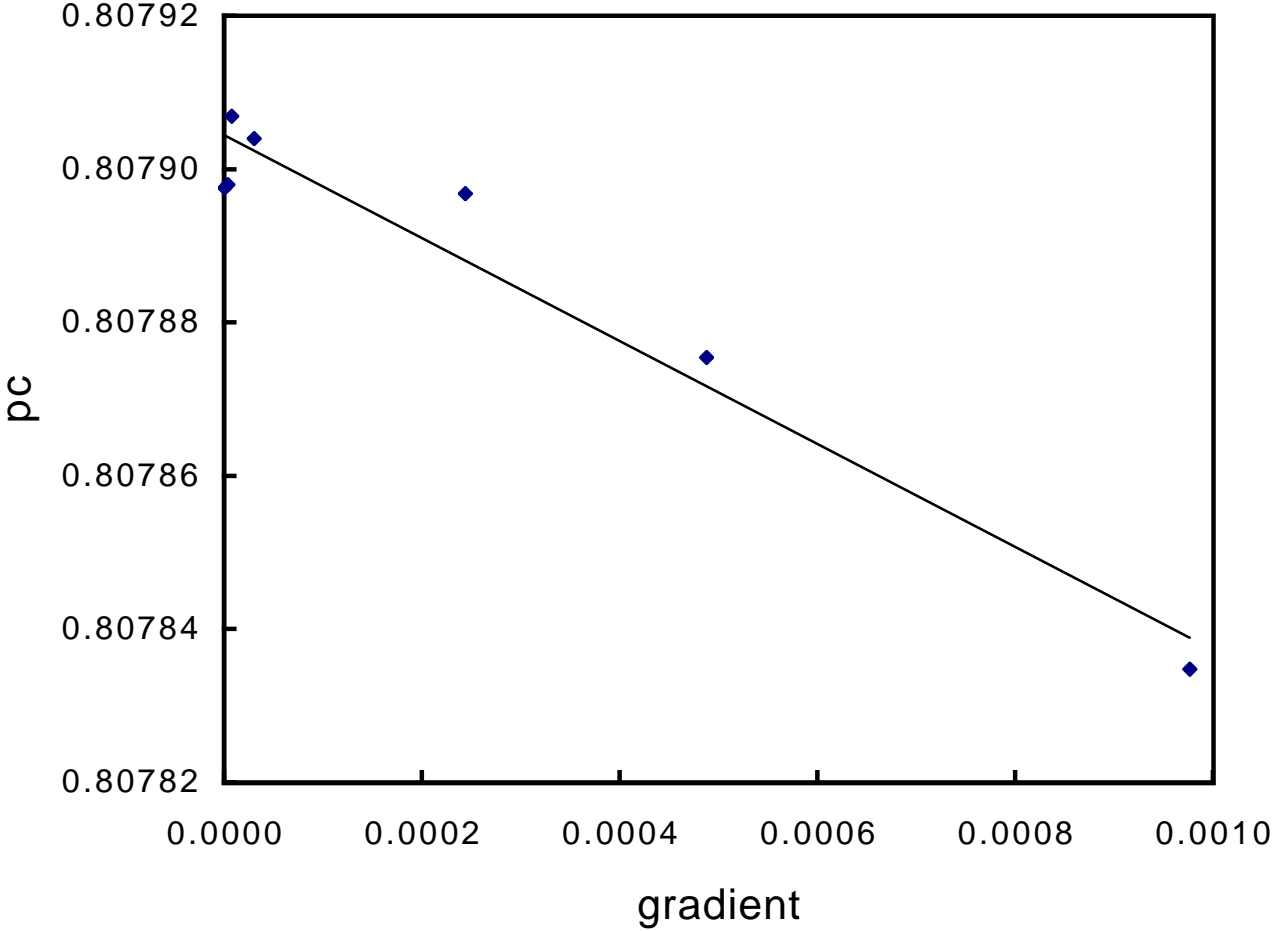


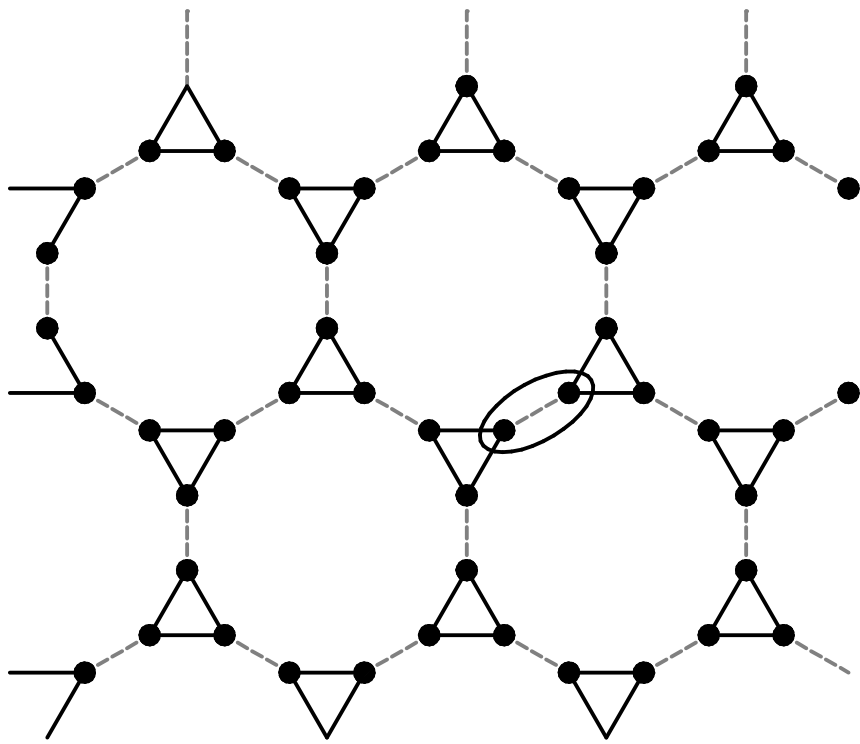
$3^2.4.3.4$



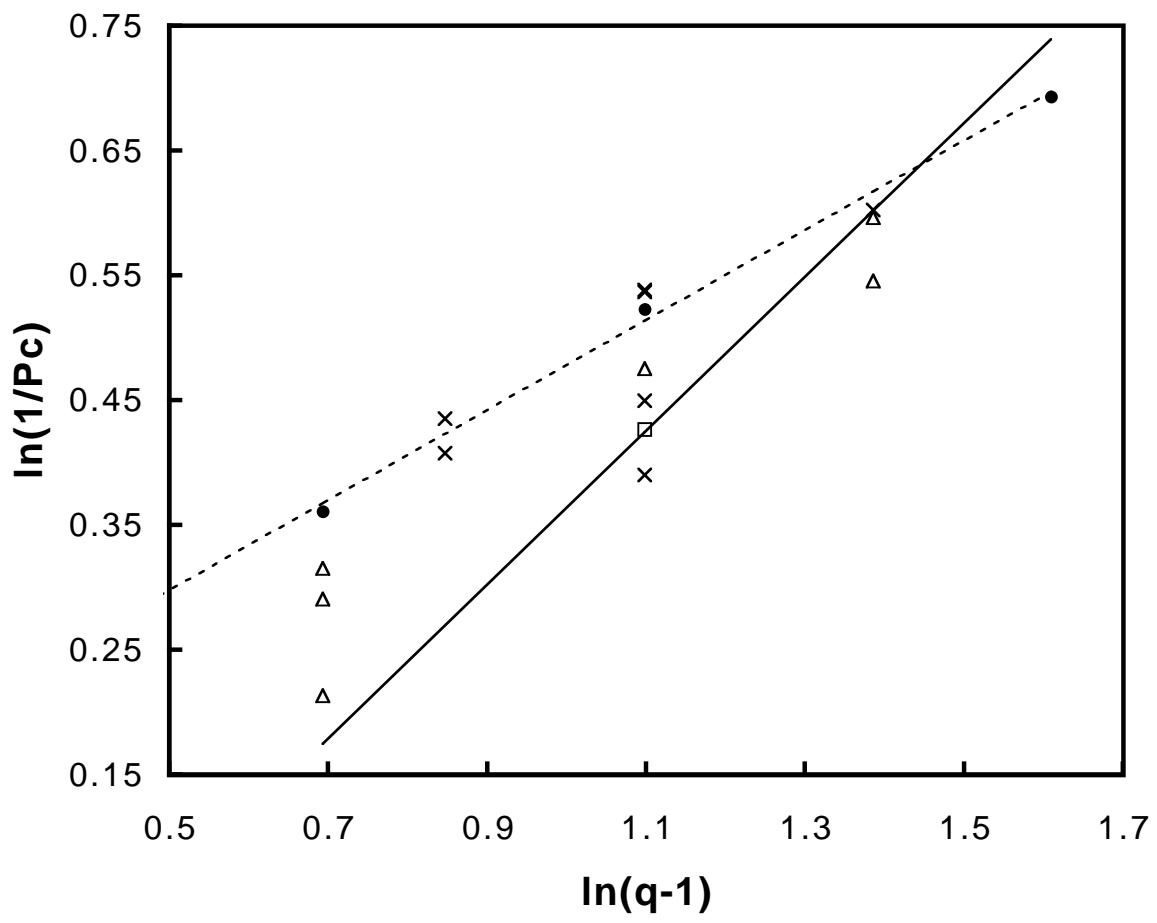
$3^3.2$

Suding-Ziff Fig. 4

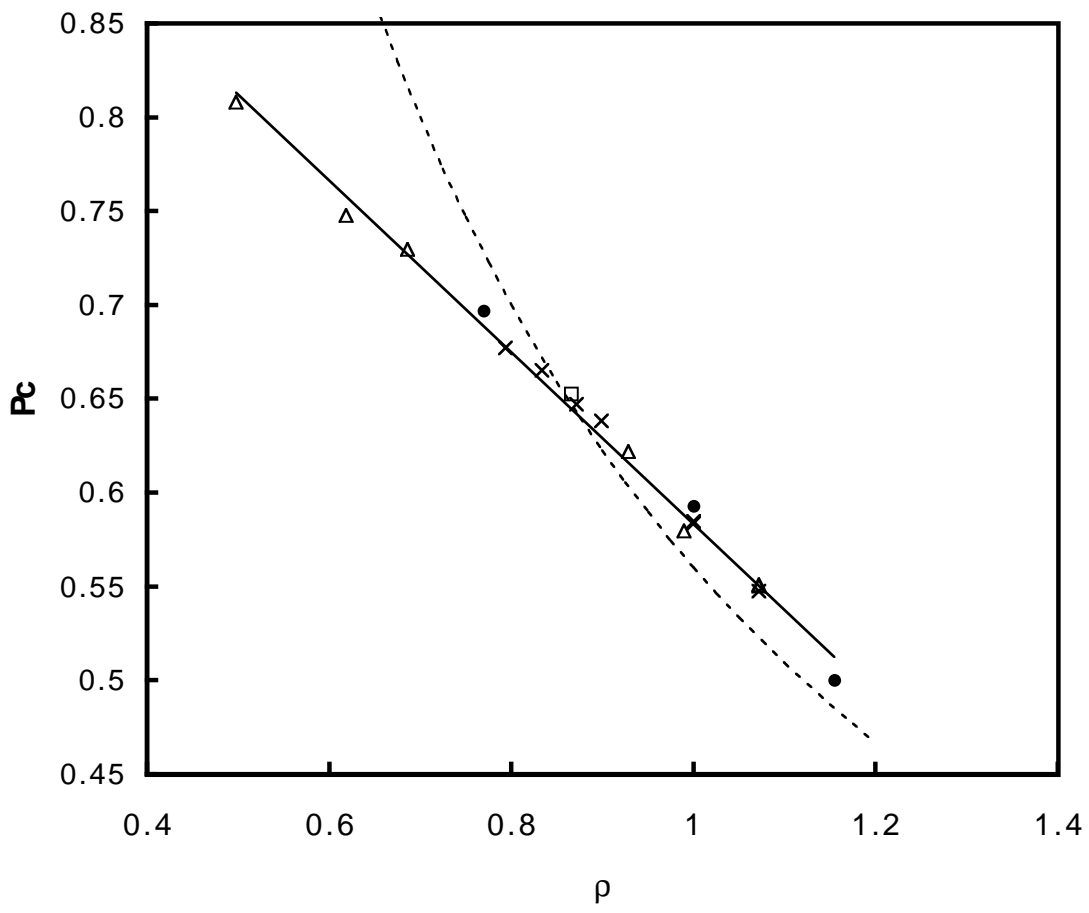




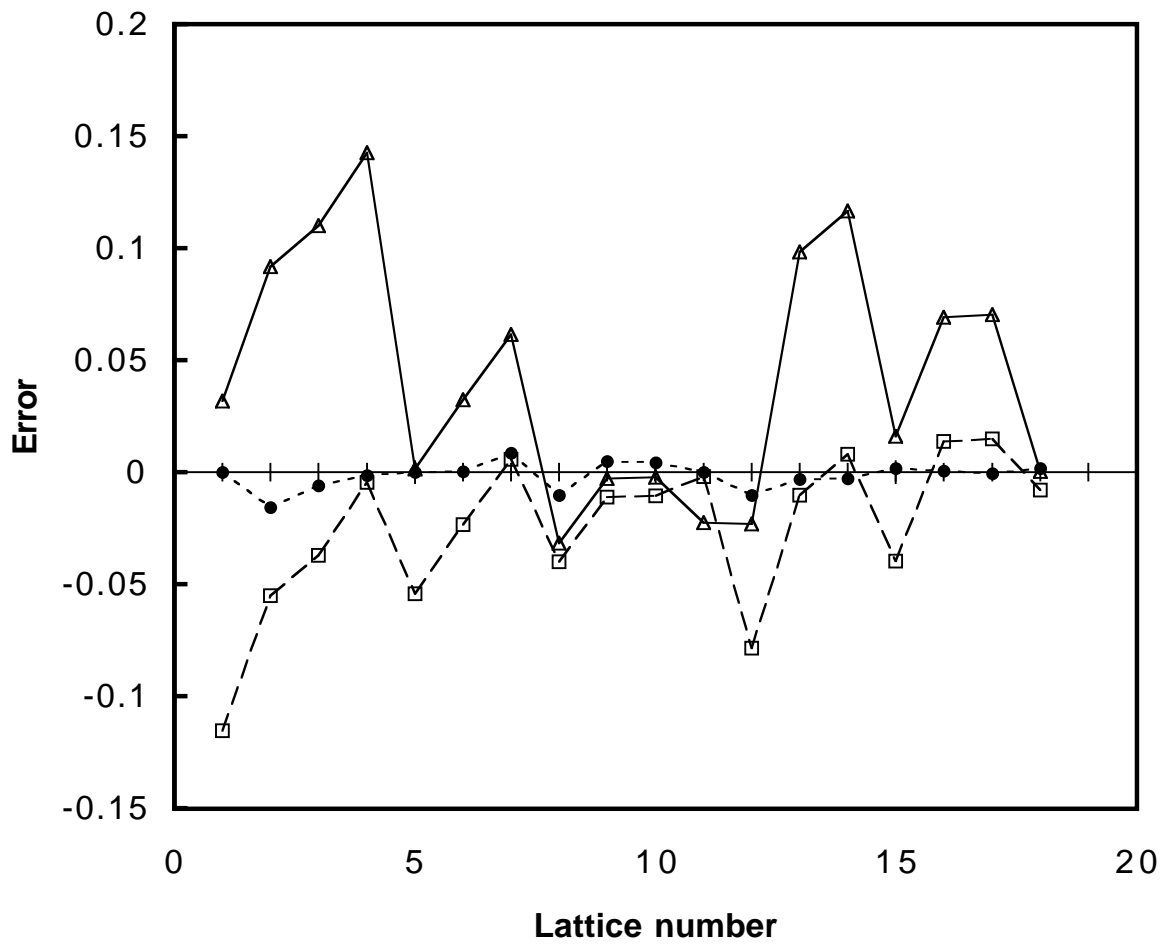
Suding and Ziff Fig. 6

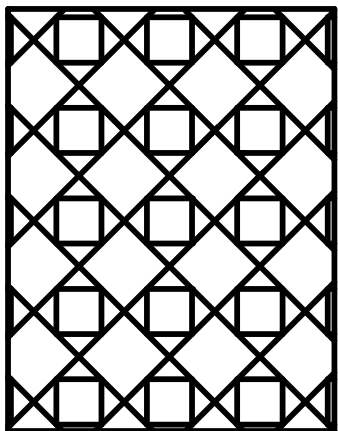


Suding and Ziff Fig. 7

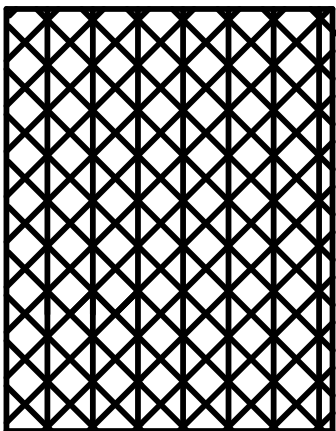


Suding Ziff Fig. 8

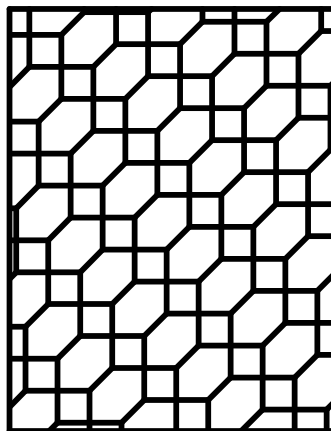




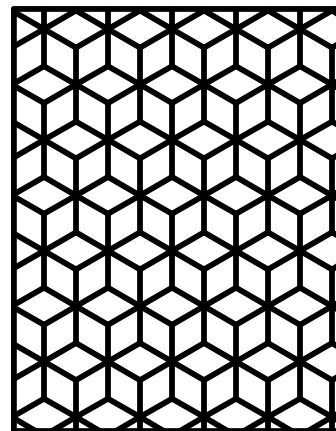
$4,8^2$ Matching



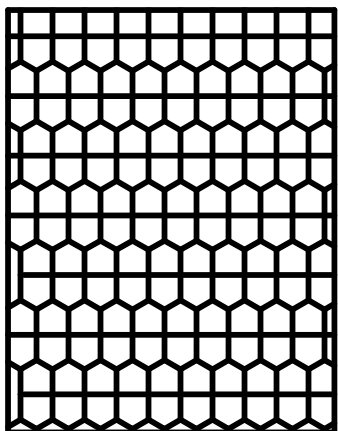
Bowtie



Bowtie Dual



Dice



Pentagonal

